Self-assembly of thiacyanine dyes in water for the synthesis of active hybrid nanofibres

Govindaswamy Shanker, Gurumurthy Hegde & Carlos Rodriguez-Abreu

⊞	View supplementary material ⟲
📅	Published online: 14 Jan 2016.
✎	Submit your article to this journal ⟲
📊	Article views: 105
🔍	View related articles ⟲
CrossMark	View Crossmark data ⟲

Taylor & Francis
Taylor & Francis Group

Self-assembly of thiacyanine dyes in water for the synthesis of active hybrid nanofibres

Govindaswamy Shanker[a,b], Gurumurthy Hegde[c] and Carlos Rodriguez-Abreu[b]

[a]Department of Studies in Chemistry, Bangalore University, Central College Campus, Bangalore, India; [b]International Iberian Nanotechnology Laboratory, Braga, Portugal; [c]BMS R & D Centre, BMS College of Engineering, Bangalore, India
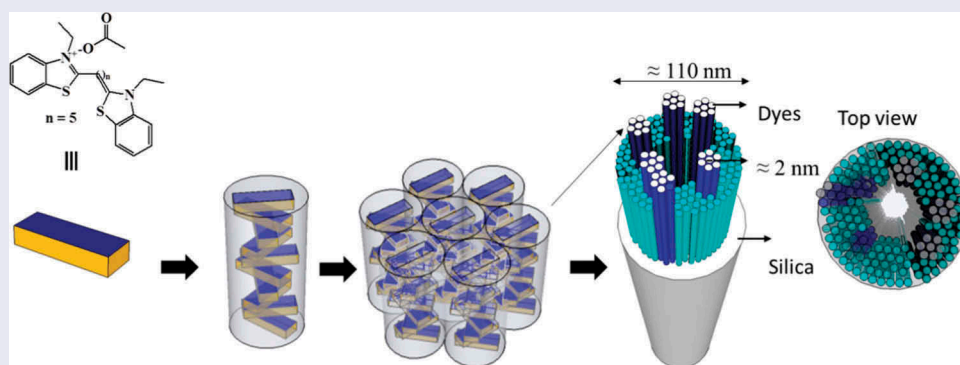
ABSTRACT

Water-soluble self-assembled nanostructures were synthesised by simple counter ion exchange of thiacyanine dyes which helps in the formation of nematic (N) and hexagonal (M) chromonic liquid-crystalline (CLCs) phases. Conjugated double bonds as central spacers connected between two benzothiazole segments affect water solubility and liquid crystal formation. Aggregation-dependent properties characterised by ultraviolet–visible, fluorescence and ^{1}H nuclear magnetic resonance spectroscopy. Sol–gel reaction of dye aggregates with silica species furnishes entangled nanotubular fibres with constant diameter and their length in excess of micrometres, having templates of pore sizes below the mesoporous range. The π–π stacked chromonic aggregate dyes are also of importance in shape selective catalysis, adsorption, desorption micro-patterned materials, and provide a significant step towards biosensor medical applications because of their water-soluble nature.

1. Introduction

Supramolecular complex molecular architectures play a vital role in the field of biological and material science.[1–10] These complex architectures form by self-assembly of smaller structural motifs and molecular sub-units through non-covalent interaction as a driving force. Liquid crystal (LC) is one such area wherein molecules self-assemble through non-covalent interactions in the formation of various kinds of LC phases.[11–14] Chromonic systems are a lyotropic counterpart wherein mesophases are formed by soluble aromatic compounds with ionic or hydrophilic groups. The molecular architectures in these systems are obtained through stacks of molecules rather than individual molecules.[15–19] A large number of aromatic compounds such as drugs, dyes and nucleic acids have a great tendency to exhibit these chromonic liquid-crystalline (CLC) phases.[20] In particular, certain classes of dyes, which are hydrophilic in nature, show a strong tendency to self-assemble into stack of columns and, at higher dye concentrations, result in ordered structures due to enthalpy as the driving force.[1–19,21–23] In addition, the column length increases at higher concentrations, mainly due to solubilising groups around the periphery of the dyes rather than at one end, and having face-to-face aggregates into columns. Disc/rod-shaped molecules with a hydrophilic nature have a greater tendency to aggregate into columns, stabilising CLC formation.[24,25]

Organisation of organic dyes into extended supra-molecular arrays is well-established and is recognised to be the result of oriented dye aggregation, arising from various dispersive forces such as π–π, cation–π, electrostatic, ion–dipole, hydrophobic and hydrogen bonding interactions between individual dye molecules.[26,27] In addition, dyes exhibiting strong fluorescence are useful as stain-tagging molecules in biological processing, particularly fluorophores with absorption and emission at longer wavelengths (600–1000 nm) that show high-sensitivity and less-background interference.[28,29] Functionalised dyes on self-assembly envisage greater utility, having multi-chromophores groups with novel optical and electronic properties.[30–32]

In recent years, organic dyes have aroused interest due to improved colouring, fluorescence, adsorption and desorption performance. Thiacyanine dyes are one such example,[33,34] wherein the dyes are made up of two benzothiazole units coupled through conjugated double chains having two nitrogen centres with one atom positively charged.

In this paper, we report the synthesis and characterisation of the self-assembly of thiacyanine dyes in water by simple counter ion exchange and their liquid-crystalline behaviour; to the best of our knowledge this will be first of its kind. We also study the effect of conjugated double bonds used as central spacers, followed by their use as templates for the preparation of CLC-based hybrid nanofibres.

2. Results and discussion

Scheme 1 shows the synthetic step for converting thiacyanine iodide into the thiacyanine acetate anion. Appropriate dyes [3,3′-diethylthiacyanine iodide (n = 1), 3,3′-diethylthiacarbocyanine iodide (n = 3), 3,3′-diethylthiadicarbocyanine iodide (n = 5), 3,3′-diethylthiatricarbocyanine iodide (n = 7)] and silver acetate (1 equiv.) were dissolved in distilled methanol (10 equiv.) and stirred at room temperature for 8 h under nitrogen atmosphere. The reaction mixture was then passed through a short column containing neutral alumina as a stationary phase. Collected solvent from the filtrates was evaporated at room temperature using nitrogen gas to achieve the thiacyanine dyes in good yield: 3,3′-diethylthiacyanine acetate (1), n = 1; 3,3′-diethylthiacarbocyanine acetate (2), n = 3; 3,3′-diethylthiadicarbocyanine acetate (3), n = 5; and 3,3′-diethylthiatricarbocyanine acetate (4), n = 7. The molecular structures of these acetate anions were determined by ^{1}H nuclear magnetic resonance (NMR) and ^{13}C NMR spectroscopy techniques (see experimental section).

Thiacyanine iodide dyes are insoluble in water, but converting the iodide anion to acetate makes these dyes soluble in water, thereby forming self-assembled nanostructures that result in formation of chromonic nematic (N) and chromonic M LC phases. In particular, dyes (2) and (3) are freely soluble in water; even at a low concentration of 0.5% (w/v), dye (2) exhibits a chromonic **N** phase with a typically characteristic Schlieren texture [11–18,21,35–37] (Figure 1(a)) with high birefringence treated on ordinary glass slides with crossed polarisers.

On increasing the dye concentration in water (3% w/v) and above, dye (2) exhibits a grainy optical texture with high birefringence typical for the M phase (Figure 1(b)).[11–18,21,38–42] This rod-shaped 3,3′-diethylthiacarbocyanine acetate (2) self-assembles into columns in the chromonic N phase with no positional order, but the same columns are rearranged in a hexagonal array furnishing the M phase showing structural similarity unlike their spatial arrangements. In addition, 3,3′-diethylthiadicarbocyanine acetate (3) exhibits a similar kind of chromonic LC behaviour; at 1% (w/v) it shows the chromonic N phase, but on increasing concentration to 5% (w/v) and above, it exhibits the M phase. Similar textural behaviour is observed for dye (3), which exhibits the chromonic N and M phases at lower concentration in water as shown in Figure 1(c) and 1(d), respectively.

The acetate anion plays a vital role in stabilising liquid-crystalline phases. This can be attributed to its
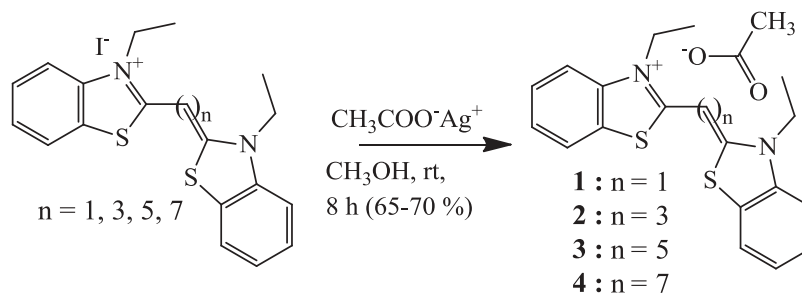
Scheme 1. Synthesis of counter anion conversion of thiacarbocyanine dyes in an alcoholic medium.
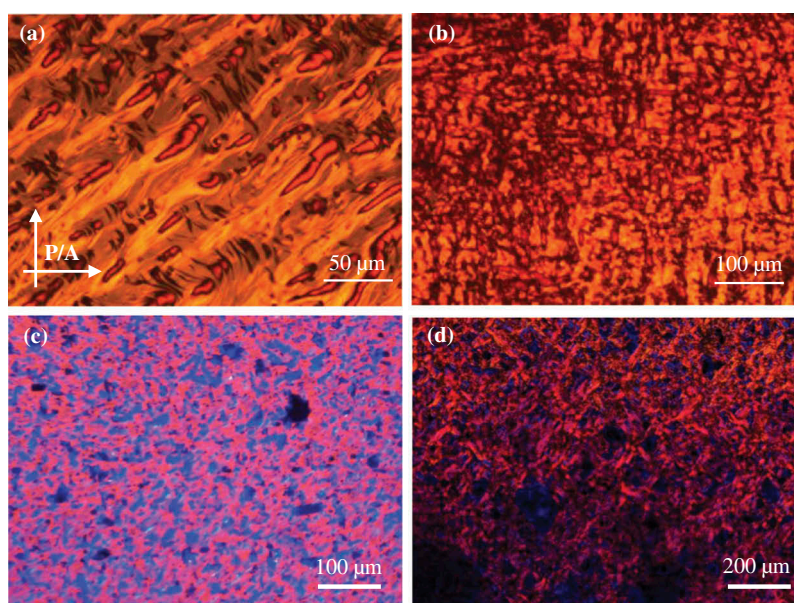
Figure 1. (colour online) Microphotographs (crossed polariser) of the textures observed at room temperature for the dyes at different concentrations in water: (a) 0.5% dye (**2**) (w/v) exhibits a chromonic N phase; (b) 5% dye (**2**) (w/v) exhibits a chromonic M phase; (c) 1% dye (**3**) (w/v) chromonic N phase; and (d) 5% dye (**3**) (w/v) chromonic M phase.

larger shape, size and flexibility compared with that of the iodide anion,[26] resulting in crystalline materials. Although the dyes with short (**1**) and long (**4**) central spacers are freely soluble in water at lower concentrations ($<10^{-4}$ M), they show strong aggregation. However, increasing the dye concentration in water does not result in chromonic liquid-crystalline phases due to partial solubility. The space filling and length-to-breath ratio in dyes (**2**) and (**3**) favours the formation of chromonic LCs; other dyes (**1** and **4**) may lack this ratio, resulting in crystalline compounds.

2.1. Aggregation of thiacyanine dyes: ultraviolet and fluorescence spectroscopy

To explore the effect of water on the aggregation of these dyes, ultraviolet–visible (UV–vis) spectra were recorded at different molar concentrations. 3,3′-Diethylthiadicarbocyanine acetate (**3**) spectra were recorded as a function of temperature. The maximum absorption was observed at λ_{max} = 523 nm at a 10^{-2} M concentration; decreases in the absorption intensity for 10^{-3} M indicated a change in aggregation state; on further dilution, the degree of aggregation changes are affected. At the lower concentration of 10^{-4} M [43] (Figure 2(b)), there is a shift in λ_{max} = 647 nm, with an additional peak at λ = 554 nm. This peak weakens for the 10^{-5} M solution followed by complete loss of aggregation on further dilution. The λ_{max} absorption peak at 647 nm towards red shifts for the 10^{-4} M solution in the whole spectra indicating the formation

of J-aggregates with a significant tilt due to repulsive electrostatic forces and the deposition of partial charges in the molecular orbitals making the π–π systems overlap.[44] An additional peak at 523 nm can be attributed to the formation of H-aggregate in the concentrated solution (Figure 2(a)). It is evident from the spectra that H-aggregation is observed at higher molar solution, followed by J-aggregation at dilute concentrations (Figure 2(a) and 2(b)).[45–50]

The morphology of thiacyanine dyes is tunable by the effect of various solvents as a result of intermolecular interactions between the solvents and the dye. A representative dye (**3**) was subjected to UV–vis analysis using methanol as solvent at different concentrations. At 10^{-2} M in methanol, dye (**3**) exhibits λ_{max} at 652 nm and, at subsequent dilute concentrations, the absorption values are decreased (Figure 2(c) and 2(d)). In comparison between (Figure 2(a) and 2(c)), an unresolved peak in the water medium observed is opposite to that of clear resolved peak in methanol. This behaviour can be attributed to the strength of the intermolecular interactions between the solvent and the dye, maximum in the case of water and reduced in methanol. This trend is expected to continue when methanol is replaced by different organic and other polar solvents.

Overall, two distinct aggregate states were evident: the thermodynamically stable H-aggregate with possibility of parallel alignment of the molecular dipole moments; and the kinetically meta-stable J-aggregation state.[51–56] The delocalised π-
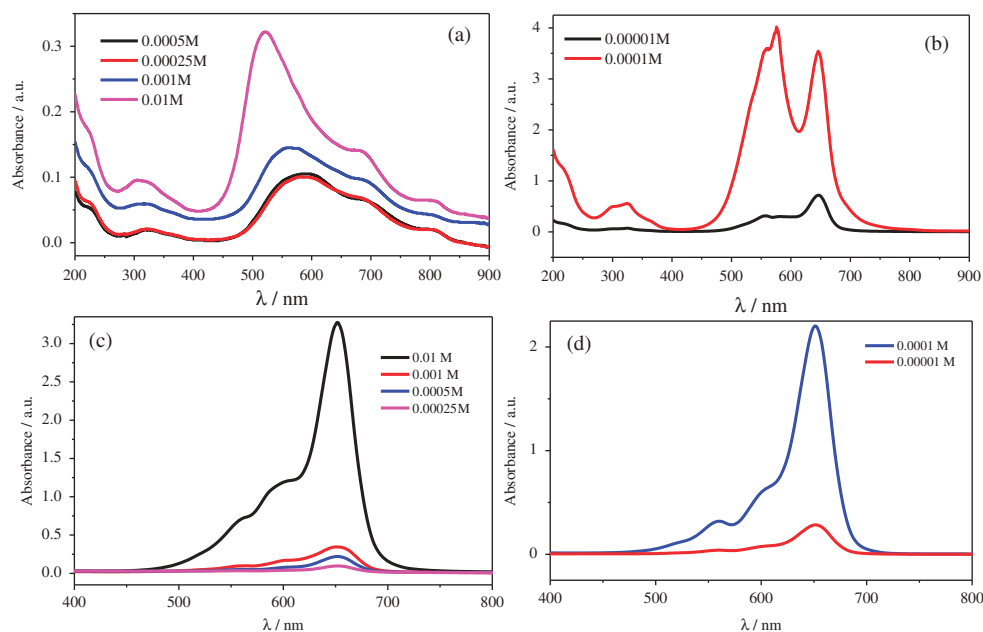
Figure 2. (colour online) UV absorption spectra of dye (**3**) in water at different molar concentrations: (a) 0.01 mm cell thickness and (b) 10 mm cell thickness. Also dye (**3**) in methanol at room temperature: (c) 0.01 mm cell thickness and (d) 10 mm cell thickness.

electrons of aromatics and the high polarisability of the dyes lead to the strong electrostatic force of attraction between the neighbouring molecules, and finally achieve a macroscopic self-assembled structure.

Intrinsic fluorescence typically occurs from aromatic molecules having strong fluorophores that occur naturally; dyes are one such example.[33,34] A representative, dye (**3**) excited at λ_{exc} = 570 nm and the relative fluorescence was recorded as a function of temperature and molar concentration in water (Figure 3). The broad fluorescence spectra observed from 625 to 750 nm are due to charged dye (**3**) itself and the decrease in intensity once again explains its aggregation at higher concentrations and breakdown on dilution. At different molar concentrations of dye (**3**) recorded as a function of temperature, on heating there is a decrease in the intensity of the peaks as a result of aggregation (Figure 3(a), 3 (c), 3(e), 3(g), 3(i)); on cooling from 65°C there is an increase in the intensity of the peaks (Figure 3(b), 3(d), 3 (f), 3(h), 3(j)), confirming the stability and reversibility of the aggregation process.

Such a reversible process can be used in sensing applications due to the morphology retention in both cycles. Analogous behaviour was observed for other dyes (**1** and **2**) in both UV and fluorescence studies, but surprisingly dye (**4**) was inert to any fluorescence excitations. These chromonic mesogens self-assemble in water to form macroscopic structures due to intermolecular interactions of aromatic rings driven by enthalpy. These interactions are presumably a combination of van der Waals forces and electrostatic attraction (π–π interaction). Longer

wavelength emission was observed for all the dyes due to effect of polarity from water, being polar themselves, the fluorophores are sensitive to solvent polarity.[57] Chromonic aggregation is isodesmic, as there is no optimum aggregation size and no critical concentration for the formation of aggregates.[58] Since these dyes are water soluble and exhibit strong fluorescence at longer wavelengths between 600 and 1000 nm, they can be used for bio-labelling in cellular uptake studies.[28,29] See the supplementary material which is available via the multimedia link on the online article webpage for more UV (Figures S1 and S4) and fluorescent (Figures S2 and S3) spectra.

2.2. Synthesis and characterisation of silica samples

The procedure used for the synthesis of silica was reminiscent of that reported in the literature.[59] A solution of 3% dye/s in aqueous 25% ammonia was prepared. Tetraethoxy ortho silicate (TEOS) (10 equiv.) was added to this solution and stirred at room temperature for 90 min and then at 70°C for an additional 90 min. The reaction mixture was filtered and the precipitate washed thoroughly with distilled ethanol to remove excess, unreacted TEOS. The resulting pure powder (60–64% yield) was further calcined in air at 600°C for 6 h with a slow heating and cooling rate of 2° C/min to produce mesoporous materials.

As evident from the reported literature,[58] chromonic LCs have a tendency to form entangled silica
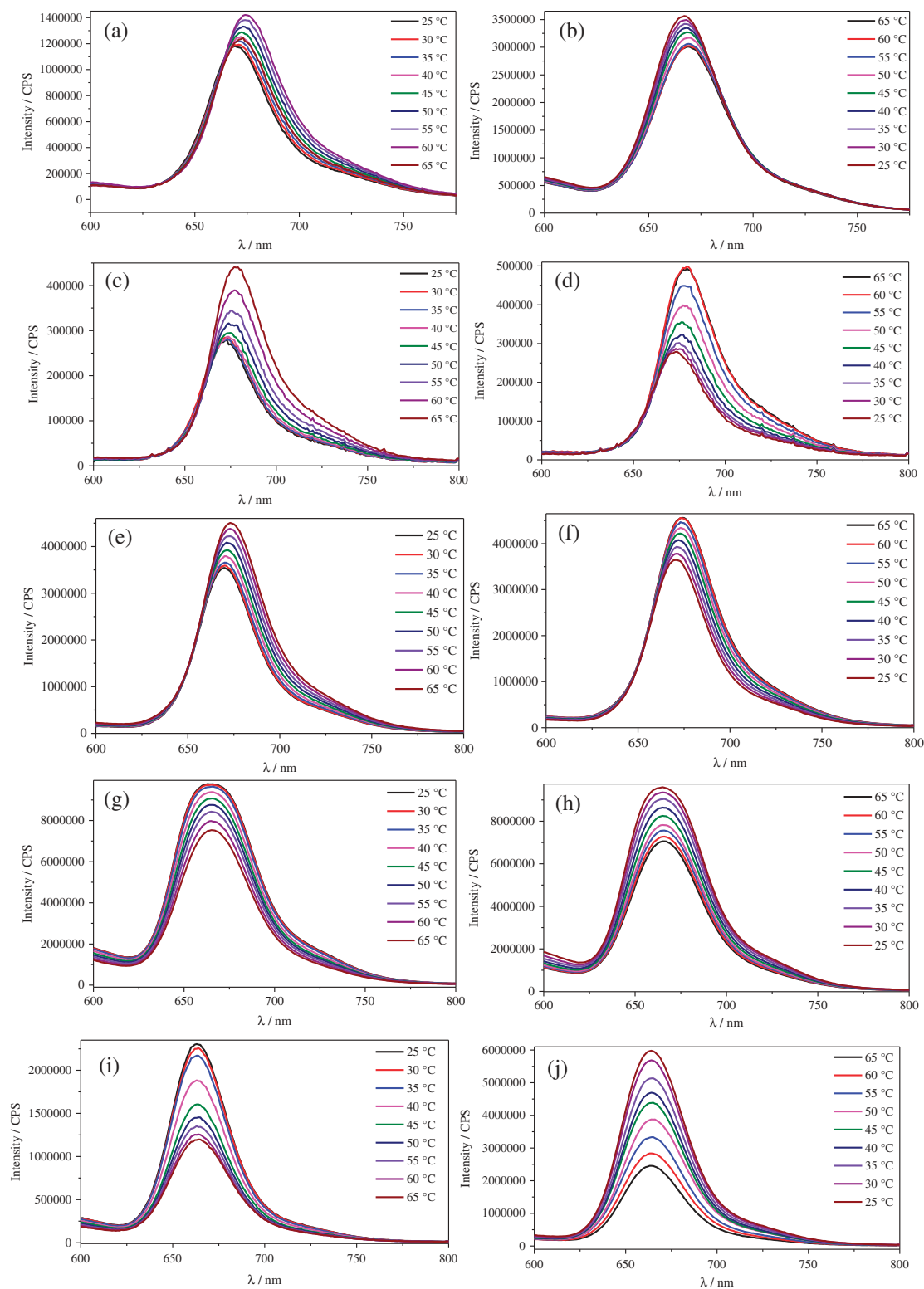
Figure 3. Fluorescence spectra of dye (**3**) in water excited at λ_{exc} = 570 nm and recorded spectra between 600 and 800 nm at room temperature for different molar concentrations: (a) 10^{-4} M heating cycles; (b) 10^{-4} M cooling cycle; (c) 5×10^{-5} M heating cycles; (d) 5×10^{-5} M cooling cycles; (e) 2.5×10^{-5} M heating cycles; (f) 2.5×10^{-5} M cooling cycles; (g) 10^{-5} M heating cycles; (h) 10^{-5} M cooling cycles; (i) 10^{-6} M heating cycles; and (j) 10^{-6} M cooling cycles. CPS, counts per second.

networks. The calcined silica of dye (**3**) shows nano-tubular fibres with a constant diameter of ≈110 nm and a length running in excess of micrometres (Figure 4(a)

and 4(b)) as evident from scanning electron microscopy (SEM) analysis. The mechanism behind this structure formation could be identical to that published
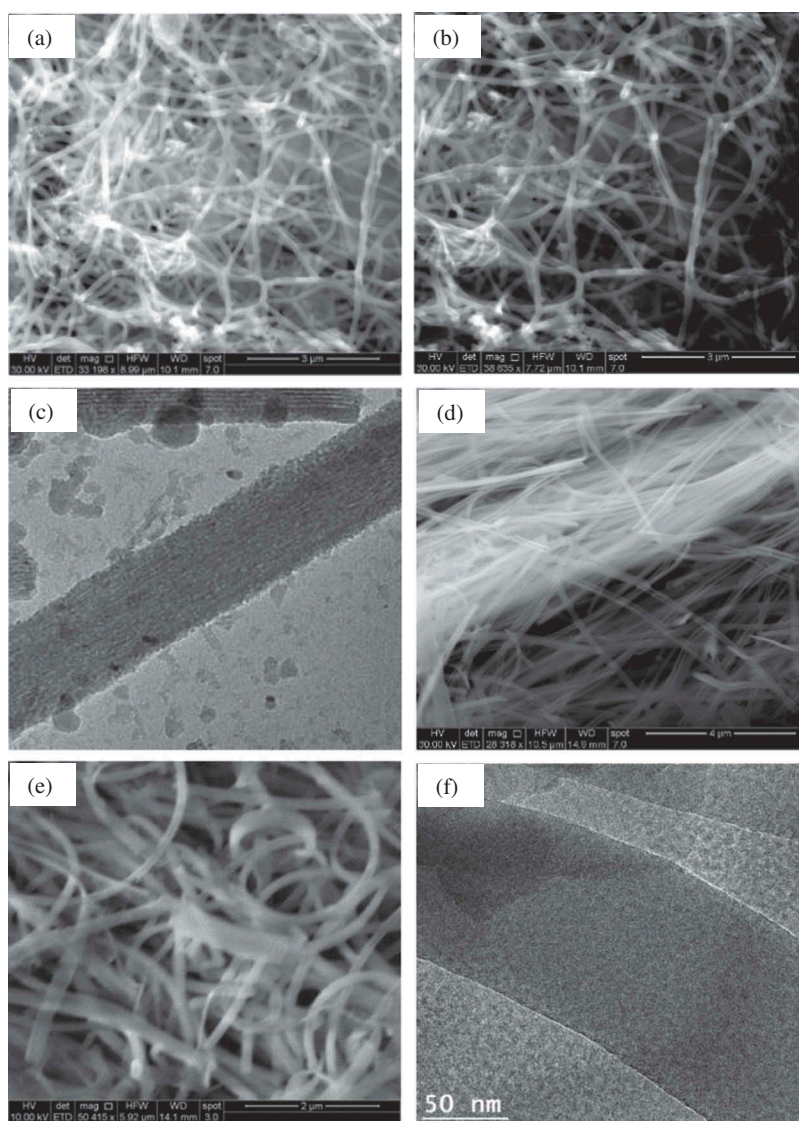
Figure 4. Electronic microscopic images: (a, b) SEM image of calcined silica of dye (**3**); (c) TEM image of calcined silica of dye (**3**); (d, e) SEM image of dye (**1**) with silica species; and (f) TEM image of dye (**1**) with silica species.

earlier.[60] The hollow nature of the tubular network is evident from the transmission electron microscopy (TEM) image (Figure 4(c)) and magnified images reveal the presence of an inside hollow structure; the walls of nanotubular fibres are made of smaller tubes with a diameter of ≈2 nm. Dye aggregates upon silica precipitation observed from TEM images are due to attractive interaction and cooperative self-assembly with silica nanoparticles during a sol–gel reaction.

Identical SEM and TEM images with more flexibility in nanotubular fibres having constant diameter with length in excess of micrometres were observed for dye (**1**) with a short methylene spacer (Figure 4(d) and 4(e)). It is also known that the thiacyanine core can be readily converted into carbon nanorods by pyrolysis; in particular, the calcined sample of dye (**3**) is suggested to generate two

different sizes of carbon nanorods by pyrolysis.[61] Dye (**4**) was not able to bind to silica using similar reaction conditions as described above.

Absorption spectra of dye (**3**) bound to silica show distinctive peaks at λ = 705 and 547 nm, indicating the presence of both J- and H-aggregates (Figure 5), even on concentration variations. The change in UV–vis spectra of the free dye (Figure 2(a) / 2(b)) compared with dye bound to silica (Figure 5) clearly indicates the formation of self-assembled nanostructures through electrostatic interaction between silica and dye.

The aggregation effect was also studied using concentration-dependent ^{1}H NMR in deuterated water for dyes (**1**), (**2**) and (**3**) with conjugated double bonds n = 1, 3, 5, respectively. The chemical shifts of dye (**1**) recorded as a function of concentration at room temperature are presented in Table 1 and the assigned
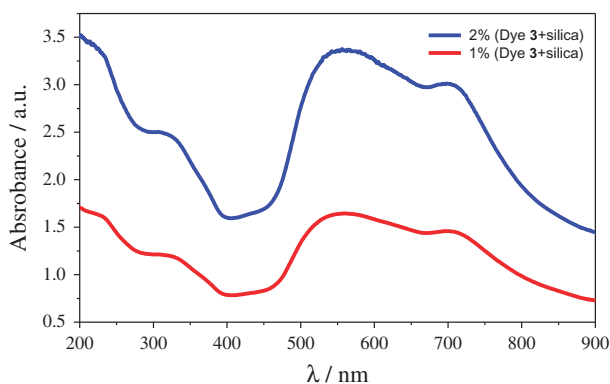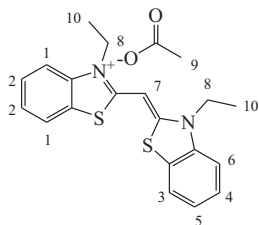
Figure 5. (colour online) UV–vis absorption spectra of dye (**3**) bound to silica at different concentrations (w/v) in water.

Table 1. Chemical shifts (δ) for dye (**1**) in deuterated water recorded as a function of concentration.

Peak (δ)	Concentration (wt %) Dye 1				
	1	0.5	0.25	0.125	0.01
1	7.511	7.597	7.676	7.750	7.883
2	7.201	7.282	7.356	7.427	7.568
3	7.139	7.228	7.311	7.387	7.531
4	7.139	7.228	7.311	7.387	7.531
5	7.052	7.136	7.209	7.276	7.400
6	7.052	7.136	7.209	7.276	7.400
7	6.031	6.113	6.186	6.253	6.382
8	4.171	4.251	4.307	4.359	4.460
9	1.941	1.940	1.939	1.939	1.939
10	1.365	1.407	1.435	1.457	1.493

peaks are in agreement with chemical structure. As the concentration of dye is decreased, there is an increase in chemical shifts (δ) of protons as a result of intermolecular interactions, especially from the aromatic rings of the benzothiazole units, which is one of the driving forces for the formation of aggregates. The signal-to-noise ratio of the spectra was poor for concentrations below 0.01%, preventing further measurements.

With respect to dye (**1**), the chemical shift (δ) difference between the highest and lowest concentrations was ≈0.390 in the case of aromatic hydrogens (H1–6) with sharp peaks showing a slow relaxation time (spin-lattice) as a result of smaller dipole–dipole

interactions. The sharp singlet observed for hydrogen (H7) with chemical shift difference = 0.350 between higher and lower concentration is less than that of aromatic hydrogens, indicates less interaction in aggregation. This trend continues for hydrogens in the methylene (H8) group. The acetate anion peak at δ 1.939 has no effect on the dilution and the chemical shift difference is negligible, emphasising the low interaction between the acetate group and the rest of the aggregated molecules. Free methyl units (H10) had a very little interaction effect in the role of aggregation. Similar behaviour was observed for two dyes (**2**) and (**3**) as described above (see Table S1 in the supplementary material which is available via the multimedia link on the online article webpage). However, due to the partial solubility of dye (**4**) in deuterated water, concentration-dependent ^{1}HNMR analysis was not possible.

Overall, chromonic aggregates lead to drastic changes in the ^{1}H NMR chemical shifts (δ) due to the shielding effect and intermolecular interaction between adjacent molecules stacked one above another in a column; there is also cross-link interaction with aromatic rings of neighbouring molecules due to the ring current.[58] Thus, a substantial chemical shift with concentrations arises in the ^{1}H NMR experiment which is reminiscent of the aforementioned UV and fluorescent analysis in confirming the aggregate process. Conjugated double bonds as a central spacer in the dyes affect the formation of CLC phases; dyes with longer and shorter conjugated double bonds (**4**) and (**1**), respectively, at 1% (w/v) concentration were partially soluble in water at room temperature, resulting in non-CLC phases.

X-ray diffraction (XRD) analysis was performed on a calcined sample of dye (**3**) bound to silica. Two low-intense peak obtained with ratio of 1: √3 corresponds to hexagonal lattice, 'd' spacing assign to 4.2 nm followed by next at 2.5 nm, whereby the ratio authenticates the hexagonal spatial arrangement. Low-intense order reflections can be attributed to the diffuse interface which also contributes to peak broadening.[26,27] (See Figure S5 in the supplementary material which is available via the multimedia link on the online article webpage.)

Based on the results of UV–vis, fluorescence, SEM, TEM, XRD and microscopic images, dye (**3**) self-assembles into nanotubular fibres having constant diameter with the inner walls made of smaller tubes as shown in the schematic diagram (Figure 6).
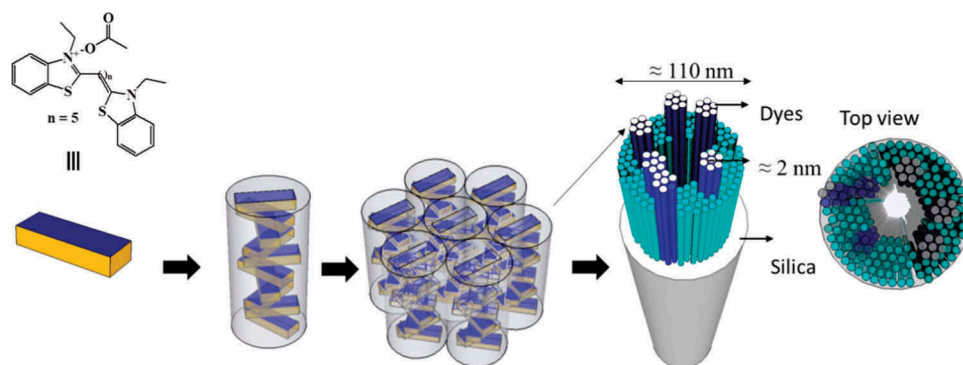
Figure 6. (colour online) Schematic representation of self-assembled nanostructure forming nanotubular fibres of dye (**3**).

3. Conclusions

Thiacyanine acetate dyes form the chromonic nematic N phase at very low concentrations (0.5%, w/v) represents first of its kind and hexagonal M liquid crystalline phases in water at higher concentrations. The acetate anion plays a vital role in stabilisation of CLC formation. In addition to ^{1}H NMR concentration-dependent analysis in deuterated water, J-aggregates observed by UV–vis and fluorescent spectroscopy experiments unambiguously confirm the stacking of these rod-shaped molecules into columns with significant tilt, [18] resulting in chromonic N and M phases at different concentrations. The conjugated double bond as a central spacer in the dyes plays a vital role in solubility and CLC formation, but a remarkable aggregation effect in water observed at lower concentrations. Sol–gel reactions of these acetate dyes with silica particles furnish an entangled network having nanotubular fibres with a constant diameter and length in excess of micrometres. Thus, these water-soluble dyes need further investigation for their applications in biological science.

4. Experimental section

All the dyes, such as 3,3′-diethylthiacyanine iodide, 3,3′-diethylthiadicarbocyanine iodide, 3,3′-diethylthiatricarbocyanine iodide and 3,3′-diethylthiacarbocyanine iodide, as well as deuterated solvents, were purchased from Sigma-Aldrich and used as such without further purification. Thin layer chromatography (TLC) was performed on precoated silica gel 60 F_{254} (Merck) plates. Ultrapure water (resistivity = 18.2 MΩ/cm) was used in all the experiments. UV–vis absorption spectra were measured using a Shimadzu UV-2550 spectrometer operating in the wavelength range 190–1100 nm. Steady-state excitation and emission fluorescence spectra were recorded with a Horiba Scientific Fluoromax-4 spectrofluorometer at a working temperature range

between −10°C and 100°C. The crude samples were purified by short flash column chromatographic technique using neutral alumina as the stationary phase. ^{1}H NMR spectra were recorded using a Bruker AMX-400 (400 MHz) spectrometer and the chemical shifts were reported in parts per million (ppm) relative to tetramethylsilane (TMS) as an internal standard. Optical polarising microscopy (OPM) was performed using a Nikon SMZ1500. Elemental microanalysis was performed using a Eurovector E300 elemental analyser. Environmental scanning electron microscopy (ESEM) images obtained using a Quanta 650 FEG (FEI) instrument at different kV switched between three vacuum modes. TEM images were collected with a Titan 200 kV ChemiStem (FEI) equipped with a Probe Cs corrector. Small angle X-ray scattering (SAXS), using an Anton Paar SAXSess MC2, is a non-destructive method in which the incoming X-ray beam interacts with the electrons of all atoms in the sample, resulting in a so-called 'scattering pattern' (X-ray intensities versus scattering angles).

4.1. Analytical data of thiacyanine dyes

(**1**): 3,3′-Diethylthiacyanine acetate. Pale greenish colour solid; yield 65% (after column chromatography); δ ^{1}H NMR (400 MHz, CD$_3$OD): δ 8.08 (d, J = 8.0 Hz, 2H, Ar), 7.83 (d, J = 8.4 Hz, 2H, Ar), 7.30 (t, J = 7.2 Hz, 2H, Ar), 7.54 (t, J = 7.6 Hz, 2H, Ar), 6.69 (s, 1H, –C**H** = CNS), 4.70 (q, J = 7.2 Hz, 4H, 2 × CH$_2$), 1.91 (s, 3H, **CH$_3$**COO⁻) 1.55 (t, J = 7.2 Hz, 6H, 2 × CH$_3$); Anal. calc'd for C$_{21}$H$_{22}$N$_2$O$_2$S$_2$: C,63.29; H, 5.56; N, 7.03. Found: C, 63.45; H, 5.04; N, 7.05.

(**2**): 3,3′-Diethylthiacarbocyanine acetate. Deep red colour solid, yield 70% (after column chromatography); δ ^{1}H NMR (400 MHz, CD$_3$OD): δ 8.00 (t, J = 12.8 Hz, 1H, –CH = C**H**–CH =), 7.84 (d, J = 8.0 Hz, 2H, Ar), 7.64 (m, 4H, Ar), 7.41 (t, J = 7.6 Hz, 2H, Ar), 6.55 (d, J = 12.4 Hz, 2H, –C**H** = CH–C**H** =), 4.42 (m, 4H,

$2 \times CH_2$), 1.91 (s, 3H, $\textbf{\textit{CH}}_3COO^-$),1.48 (t, J = 7.2 Hz, 6H, $2 \times CH_3$); ^{13}C NMR (100 MHz, CD$_3$OD) δ 181.39, 166.48, 148.47, 142.34, 129.39, 129.29, 127.89, 126.91, 126.57, 123.86, 122.40, 114.16, 112.57, 99.45, 42.82, 24.01, 12.93; Anal. calc'd for $C_{23}H_{24}N_2O_2S_2$: C, 65.06; H, 5.70; N, 6.60. Found: C, 65.05; H, 5.40; N, 6.44.

(**3**): 3,3′-Diethylthiadicarbocyanine acetate. Blue colour solid; yield 72% (after column chromatography); δ ^1H NMR (400 MHz, CD$_3$OD): δ 7.82 (d, J = 7.6 Hz, 2H, Ar), 7.70 (d, J = 12.8 Hz, 2H, Ar), 7.62 (m, 4H, Ar), 7.42 (m, 2H, $-C\textbf{\textit{H}} = C\textbf{\textit{H}}-$), 6.59 (m, 1H, $-C\textbf{\textit{H}} = CNS$), 6.47 (m, 2H, $-C\textbf{\textit{H}} = C\textbf{\textit{H}}-$), 4.43 (m, 4H, $2 \times CH_2$), 1.93 (s, 3H, $\textbf{\textit{CH}}_3COO^-$),1.48 (m, 6H, $2 \times CH_3$); ^{13}C NMR (100 MHz, CD$_3$OD) δ 179.40, 164.91, 151.90, 142.25, 129.27, 129.15, 127.09, 126.43, 126.13, 123.69, 122.27, 114.05, 113.75, 100.95, 99.53, 42.64, 23.72, 13.00; Anal. calc'd for $C_{25}H_{26}N_2O_2S_2$: C, 66.63; H, 5.82; N, 6.22. Found: C, 66.51; H, 5.98; N, 6.43.

(**4**): 3,3′-Diethylthiatricarbocyanine acetate. Olive green colour solid; yield 65% (after column chromatography); δ ^1H NMR (400 MHz, CD$_3$OD): δ 7.82 (m, 2H, Ar), 7.59 (m, 6H, Ar), 7.56 (m, 1H, $-C\textbf{\textit{H}} = CNS$), 7.52 (m, 3H, $-C\textbf{\textit{H}} = C\textbf{\textit{H}}-C\textbf{\textit{H}} =$), 6.49 (m, 3H, $= C\textbf{\textit{H}}-C\textbf{\textit{H}} = C\textbf{\textit{H}}-$), 4.41 (m, 4H, $2 \times CH_2$), 1.99 (s, 3H, $\textbf{\textit{CH}}_3COO^-$),1.46 (m, 6H, $2 \times CH_3$); Anal. calc'd for $C_{27}H_{28}N_2O_2S_2$: C, 68.03; H, 5.92; N, 5.88. Found: C, 68.05; H, 5.83; N, 5.79.

Acknowledgements

Disclosure statement

No potential conflict of interest was reported by the authors.

References

[1] Lehn J-M. Supramolecular chemistry – scope and perspectives molecules, supermolecules, and molecular devices. Angew Chem Int Ed Engl. 1988;27:89–112. DOI:10.1002/anie.198800891.

[2] Ikkala O, Ten Brinke G. Functional materials based on self-assembly of polymeric supramolecules. Science. 2002;295:2407–2409. DOI:10.1126/science.1067794.

[3] Shimizu T, Masuda M, Minamikawa H. Supramolecular nanotube architectures based on amphiphilic molecules. Chem Rev. 2005;105:1401–1444. DOI:10.1021/cr030072j.

[4] Lehn J-M. Supramolecular chemistry: concepts and perspectives. Weinheim: Wiley-VCH; 1995.

[5] Lehn J-M. Toward self-organization and complex matter. Science. 2002;295:2400–2403. DOI:10.1126/science.1071063.

[6] Diederich FN. 40 years of supramolecular chemistry. Angew Chem Int Ed. 2007;46:68–69. DOI:10.1002/(ISSN)1521-3773.

[7] Kato T, Mizoshita N, Kishimoto K. Functional liquid-crystalline assemblies: self-organized soft materials. Angew Chem Int Ed. 2006;45:38–68. DOI:10.1002/(ISSN)1521-3773.

[8] Gin DL, Lu X, Nemade PR, et al. Recent advances in the design of polymerizable lyotropic liquid-crystal assemblies for heterogeneous catalysis and selective separations. Adv Funct Mater. 2006;16:865–878. DOI:10.1002/adfm.200500280.

[9] Ko YH, Kim E, Hwang I, et al. Supramolecular assemblies built with host-stabilized charge-transfer interactions. Chem Commun. 2007;2007:1305–1315. DOI:10.1039/B615103E.

[10] Kivala M, Boudon C, Gisselbrecht J-P, et al. Charge-transfer chromophores by cycloaddition–retro-electro-cyclization: multivalent systems and cascade reactions. Angew Chem Int Ed. 2007;46:6357–6360. DOI:10.1002/anie.v46:33.

[11] Goodby JW, Saez IM, Cowling SJ, et al. Transmission and amplification of information and properties in nanostructured liquid crystals. Angew Chem Int Ed. 2008;47:2754–2787. DOI:10.1002/(ISSN)1521-3773.

[12] Kato T. Self-assembly of phase-segregated liquid crystal structures. Science. 2002;295:2414–2418. DOI:10.1126/science.1070967.

[13] Whitesides GM, Grzybowski B. Self-assembly at all scales. Science. 2002;295:2418–2421. DOI:10.1126/science.1070821.

[14] Ringsdorf H, Schlarb B, Venzmer J. Molecular architecture and function of polymeric oriented systems: models for the study of organization, surface recognition, and dynamics of biomembranes. Angew Chem Int Ed Engl. 1988;27:113–158. DOI:10.1002/(ISSN)1521-3773.

[15] Lydon J. Chromonic liquid crystal phases. Curr Opin Colloid Interface Sci. 1998;3:458–466. DOI:10.1016/S1359-0294(98)80019-8.

[16] Lydon J. Chromonics. In: Demus D, Goodby J, Gray GW, et al., editors. Handbook of liquid crystals. Weinheim: Wiley-VCH; 1998. Vol. 2B, Chapter XVIII. p. 981–1008.

[17] Attwood TK, Lydon J, Hall C, et al. The distinction between chromonic and amphiphilic lyotropic mesophases. Liq Cryst. 1990;7:657–668. DOI:10.1080/02678299008036749.

[18] Attwood TK, Lydon J, Jones F. The chromonic phases of dyes. Liq Cryst. 1986;1:499–507. DOI:10.1080/02678298608086274.

[19] Lydon J. Chromonic liquid crystalline phases. Liq Cryst. 2011;38:1663–1681. DOI:10.1080/02678292.2011.614720.

[20] Chang S-WT, Huang L. Chromonic liquid crystals: properties and applications as functional materials. Chem Commun. 2008;2008:1957–1967. DOI:10.1039/b714319b.

[21] Tschierske C. Liquid crystal engineering – new complex mesophase structures and their relations to polymer

morphologies, nanoscale patterning and crystal engineering. Chem Soc Rev. 2007;36:1930–1970. DOI:10.1039/b615517k.

[22] Lydon J. Chromonic mesophases. Curr Opin Colloid Interface Sci. 2004;8:480–490. DOI:10.1016/j.cocis.2004.01.006.

[23] Lydon J. A personal history of the early days of chromonics. Liq Cryst Today. 2007;16:13–27. DOI:10.1080/14645180701876080.

[24] Cox JSG, Woodard GD, McCrone WC. Solid-state chemistry of cromolyn sodium (disodium cromoglycate). J Pharm Sci. 1971;60:1458–1465. DOI:10.1002/(ISSN)1520-6017.

[25] Hartshorne NH, Woodard GD. Mesomorphism in the system disodium chromoglycae–water. Mol Cryst Liq Cryst. 1973;23:343–368. DOI:10.1080/15421407308083381.

[26] Rodriguez-Abreu C, Torres CA, Tiddy GJT. Chromonic liquid crystalline phases of pinacyanol acetate: characterization and use as templates for the preparation of mesoporous silica nanofibers. Langmuir. 2011;27:3067–3073. DOI:10.1021/la1048024.

[27] Rodriguez-Abreu C, Torres CA, Solans C, et al. Characterization of perylene diimide dye self-assemblies and their use as templates for the synthesis of hybrid and supermicroporous nanotubules. ACS Appl Mater Interfaces. 2011;3:4133–4141. DOI:10.1021/am201016m.

[28] Frangioni JV, Onishi S, inventors. Serum albumin conjugated to fluorescent substances for imaging. United States patent US 082423A2; 2005.

[29] Jose J, Burgess K. Benzophenoxazine-based fluorescent dyes for labeling biomolecules. Tetrahedron. 2006;62:11021–11037. DOI:10.1016/j.tet.2006.08.056.

[30] Iverson IK, Casey SM, Seo W, et al. Controlling molecular orientation in solid films via self-organization in the liquid-crystalline phase. Langmuir. 2002;18:3510–3516. DOI:10.1021/la011499t.

[31] Han KQ, Xianyu HQ, Eakin J, et al. Orientationally ordered and patterned discotic films and carbon films from liquid crystal precursors. Carbon. 2005;43:407–415. DOI:10.1016/j.carbon.2004.10.002.

[32] Sousa ME, Cloutier SG, Jian KQ, et al. Patterning lyotropic liquid crystals as precursors for carbon nanotube arrays. Appl Phys Lett. 2005;87:173115. DOI:10.1063/1.2108111.

[33] Jia Z, Ma Y, Yang W, et al. Effects of bad solvents on thiatricarbocyanine particles formation. Colloids Surf A Physicochem Eng Asp. 2006;272:164–169. DOI:10.1016/j.colsurfa.2005.07.025.

[34] Sergio L, Rooy D, Das S, et al. Ionic liquid mixtures—variations in physical properties and their origins in molecular structure. J Phys Chem. C. 2012;16:8251–8258.

[35] Iverson IK, Tam-Chang S-W. Cascade of molecular order by sequential self-organization, induced orientation, and order transfer processes. J Am Chem Soc. 1999;121:5801–5802. DOI:10.1021/ja983803j.

[36] Iverson IK, Casey SM, Seo W, et al. Controlling molecular orientation in solid films via self-organization in the liquid-crystalline phase. Langmuir. 2002;18:3510–3516. DOI:10.1021/la011499t.

[37] Tam-Chang S-W, Iverson IK, Helbley J. Study of the chromonic liquid-crystalline phases of bis-(N, N-diethylaminoethyl)perylene-3,4,9,10-tetracarboxylic diimide dihydrochloride by polarized optical microscopy and 2H NMR spectroscopy. Langmuir. 2004;20:342–347. DOI:10.1021/la030256t.

[38] Tam-Chang S-W, Helbley J, Carson TD, et al. Template-guided organization of chromonic liquid crystals into micropatterned anisotropic organic solids. Chem Commun. 2006;2006:503–505. DOI:10.1039/B508220J.

[39] Sandqvist H. Anisotropic aqueous solution. Ber Dtsch Chem Ges. 1915;48:2054–2055. DOI:10.1002/cber.191504802105.

[40] Turner JE, Lydon J. Chromonic mesomorphism: the range of lyotropic discotic phases. Mol Cryst Liq Cryst Lett. 1988;5:93–99.

[41] Lydon J. New models for the mesophases of disodium cromoglycate (INTAL). Mol Cryst Liq Cryst Lett. 1980;64:19–24. DOI:10.1080/01406568008072650.

[42] Attwood TK, Lydon J. Lyotropic mesophase formation by anti-asthmatic drugs. Mol Cryst Liq Cryst. 1984;108:349–357. DOI:10.1080/00268948408078686.

[43] A cell of 10 mm thick was used to record the UV spectra even at this dilute concentration.

[44] Kirstein S, Daehne S. J-aggregates of amphiphilic cyanine dyes: Self-organization of artificial light harvesting complexes. Int J Photoenergy. 2006;20363:1–21.

[45] West W, Pearce S, Grum F. Stereoisomerism in cyanine dyes–meso-substituted thiacarbocyanines. J Phys Chem. 1967;71:1316–1326. DOI:10.1021/j100864a021.

[46] West W, Pearce S. The dimeric state of cyanine dyes. J Phys Chem. 1965;69:1894–1903. DOI:10.1021/j100890a019.

[47] Bayliss NS. The effect of the electrostatic polarization of the solvent on electronic absorption spectra in solution. J Phys Chem. 1950;18:292–296. DOI:10.1063/1.1747621.

[48] West W, Geddes AL. The effects of solvents and of solid substrates on the visible molecular absorption spectrum of cyanine dyes. J Phys Chem. 1964;68:837–847. DOI:10.1021/j100786a023.

[49] Mishra A, Behera RK, Behera PK, et al. Cyanines during the 1990s: a review. Chem Rev. 2000;100:1973–2012. DOI:10.1021/cr990402t.

[50] Chen G, Sasabe H, Lu W, et al. J-aggregation of a squaraine dye and its application in organic photovoltaic cells. J Mater Chem C. 2013;1:6547–6552. DOI:10.1039/c3tc31243g.

[51] Wojtyk J, McKerrow A, Kazmaier P, et al. Quantitative investigations of the aggregation behaviour of hydrophobic anilino squaraine dyes through UV/vis spectroscopy and dynamic light scattering. Can J Chem. 1999;77:903–912. DOI:10.1139/v99-073.

[52] Liang K, Law K-Y, Whitten DG. Multiple aggregation of surfactant squaraines in Langmuir–Blodgett films and in DMSO–water mixtures. J Phys Chem. 1994;98:13379–13384. DOI:10.1021/j100101a043.

[53] Wurthner F, Kaiser TE, Saha-Moller CR. J-aggregates: from serendipitous discovery to supramolecular engineering of functional dye materials. Angew

Chem Int Ed. 2011;50:3376–3410. DOI:10.1002/anie.201002307.

[54] Kaiser TE, Wang H, Stepanenko V, et al. Supramolecular construction of fluorescent J-aggregates based on hydrogen-bonded perylene dyes. Angew Chem Int Ed. 2007;46:5541–5544. DOI:10.1002/anie.200701139.

[55] Das A, Ghosh S. Contrasting self-assembly and gelation properties among bis-urea-and bis-amide-functionalised dialkoxynaphthalene (DAN) π systems. Chem Eur J. 2010;16:13622–13628. DOI:10.1002/chem.201002208.

[56] Molla MR, Ghosh S. Hydrogen-bonding-mediated J-aggregation and white-light emission from a remarkably simple, single-component, naphthalenediimide chromophore. Chem Eur J. 2012;18:1290–1294. DOI:10.1002/chem.v18.5.

[57] Mataga N, Kaifu Y, Koizumi M. Solvent effects upon fluorescence spectra and the dipole moments of excited molecules. Bull Chem Soc Jpn. 1956;29:465–470. DOI:10.1246/bcsj.29.465.

[58] Lydon J. Chromonic review. J Mater Chem. 2010;20:10071–11099. DOI:10.1039/b926374h.

[59] Di Renzo F, Cambon H, Dutarte R. A 28-year-old synthesis of micelle-templated mesoporous silica. Microporous Mater. 1997;10:283–286. DOI:10.1016/S0927-6513(97)00028-X.

[60] Sinks LE, Rybtchinski B, Iimura M, et al. Self-assembly of photofunctional cylindrical nanostructures based on perylene-3,4:9,10-bis(dicarboximide). Chem Mater. 2005;17:6295–6303. DOI:10.1021/cm051461s.

[61] Yi Z, Han X, Ai C, et al. Reversible lithium intercalation in disordered carbon prepared from 3,4,9,10-perylenetetracarboxylic dianhydride. J Solid State Electrochem. 2008;12:1061–1066. DOI:10.1007/s10008-007-0427-9.